

# Parametric Study of Confined Turbulent Impinging Slot Jets upon a Flat Plate

A. M. Tahsini, and S. Tadayon Mousavi

**Abstract**—In the present paper, a numerical investigation has been carried out to classify and clarify the effects of paramount parameters on turbulent impinging slot jets. The effects of nozzle's exit turbulent intensity, distance between nozzle and impinging plate are studied at Reynolds number 5000 and 20000. In addition, the effect of Mach number that is varied between 0.3-0.8 at a constant Reynolds number 133000 is investigated to elucidate the effect of compressibility in impinging jet upon a flat plate. The wall that is located at the same level with nozzle's exit confines the flow. A compressible finite volume solver is implemented for simulation the flow behavior. One equation Spalart-Allmaras turbulent model is used to simulate turbulent flow at this study. Assessment of the Spalart-Allmaras turbulent model at high nozzle to plate distance, and giving enough insights to characterize the effect of Mach number at high Reynolds number for the complex impinging jet flow are the remarkable results of this study.

**Keywords**—Impinging jet, Numerical simulation, Turbulence.

## I. INTRODUCTION

COOLING/heating of metal plates, cleaning of iced aircraft wings, cooling of leading edge in turbine blades and combustion chamber walls, tempering of glass, cooling of electronic equipment, age hardening and safety requirements in the storage of cylinders containing liquefied gas are some of the common examples of many applications of favorable impinging jets physics at industry. The flow structure of unconfined impinging jets is divided to three main regions: free jet region, stagnation region and wall jet region. After jet exits from the nozzle's inlet, it releases into surrounding ambient and free jet begins developing by entrainment of surrounding fluid. Depending on the nozzle to surface distance, before jet impinges upon plate, the jet can pass three different zones, developed free jet's formation containing potential core zone, developing zone and developed zone. The second region is stagnation region where the jet strikes to the target wall and deflects. Maximum Nusselt number is observed in the stagnation point or the surrounding point due to the formation of thin thermal boundary layer in this region. After impinging, the jet deflects and grows as a wall jet over target plate. Confined impinging jets have these three global regions, but the upper wall that is in the same level with the nozzle's exit restricts entrainment of jets, so the length of potential core in confined jets is more than free jets; therefore the Nusselt number has experienced greater amount related to

unconfined jet in the same condition for laminar impinging jets. In addition, reducing the entrainment, the turbulence intensity is lower when the jet impacts on the surface related to unconfined jet. Deciding which parameter is dominant at distribution of Nusselt number for confined case in respect to unconfined one, is related to Reynolds number, nozzle to plate distance and other important parameters in turbulent impinging jet physics.

Many investigations have been carried out to illustrate the paramount parameters at complex turbulent impinging jets. Viskanta [1] gathered a whole and comprehensive review of numerical and experimental researches that had been done before. Gardon and Akfirat [2] experimentally measured the heat transfer of a submerged impinging jets and discussed the Nusselt number behavior by considering some parameters like nozzle to surface distance, Reynolds number and turbulence intensity of jet both at the nozzle's exit and measured intensity during jet's trajectory. Furthermore, local Nusselt number of plane and round turbulent impinging jets were compared to clarify differences between these two nozzle shapes. Baydar [3] experimentally investigated pressure coefficient distribution over impinging flat plate for single and double impinging jets at Reynolds number up to 10000. Formed sub-atmospheric region on the flat plate was observed for both single and double impinging jets at dimensionless nozzle to plate distance 2, and strengthen of this region was enhanced by increasing Reynolds number. The author concluded that a linkage exists between this sub-atmospheric region and second peak of Nusselt number over impinging flat plate. Behnia et al. [4] simulated flow behavior in axisymmetric turbulent impinging jet by using of  $v^2-f$  turbulent model. They compared  $v^2-f$  simulation result with low Reynolds  $k-\epsilon$  model and verified the  $v^2-f$  performance. Based on the present results, low Reynolds  $k-\epsilon$  model over-predicts Nusselt number especially at stagnation region due to production of high turbulent kinetic energy. Park et al. [5] simulated turbulent impinging slot jet with  $k-\omega$  model and SUPG (SIMPLE-based segregated streamline upwind Petrov-Galerkin) discretization method. Simulated results are in good agreement with experimental result at low Reynolds number, but the accuracy of position and magnitude prediction of Nusselt number second peak is diminished with increasing Reynolds number. They explained that these discrepancies are arisen from two-dimensional simulation. O'Donovan and Murray [6] experimentally investigated the mean and fluctuation of axial and radial velocity and Nusselt number for an unconfined round jet. They concluded the position of the second peak of Nusselt number that is observed at low nozzle to impinging plate distance, moves to larger distance related to stagnation

A. M. Tahsini, Assistant Professor, Aerospace Research Institute, Tehran, Iran; (e-mail: a\_m\_tahsini@yahoo.com)

S. Tadayon Mousavi, M. Sc. Student, Aerospace Research Institute, Tehran, Iran.

point by increasing nozzle to surface distance and its magnitude is decreased. In addition, they indicated that the position of secondary peak of Nusselt number coincides with the position of velocity fluctuation peak, especially axial velocity fluctuations. However, they didn't observe any peak for velocity fluctuation at high nozzle to surface distance, so they postulated that some other parameters rather velocity fluctuation are responsible for second peak of Nusselt number at higher nozzle to surface distance. Beaubert and Viazzo [7] numerically simulated confined impinging slot jet at Reynolds numbers 3000-7500 and at a fixed dimensionless nozzle to surface 10 with LES method. Formation of vortices at free jet shear layer before impinging upon flat plate is shown and discussed at this study. In addition, this simulation clarifies the existence of counter rotating vortices at both side of the symmetry plane. Kubacki and Dick [8] studied flow characteristics at confined impinging slot jet at Reynolds number 13500, 20000 and dimensionless nozzle to surface 4, 9.2 and 20 by implementation of hybrid RANS/LES method. They compared their results with  $k-\omega$  and experimental data. At low nozzle to surface distance,  $k-\omega$  can predict flow and heat transfer behavior with the same accuracy related to hybrid RANS/LES method because the impinging plate is located at the distance that is shorter than potential core of the jet, so jet is laminar at its axis. On the contrary, at high nozzle to surface distance, RANS over-predicts the length of the potential core and under-predict the turbulent kinetic energy at the jet shear layer; hence, its prediction is not satisfied and hybrid RANS/LES is preferred at larger distance because of reasonable correspondence results with experiment. Hattori and Nagano [9] simulated flow characteristics of confined impinging plane jet by DNS at Reynolds number 4560 and dimensionless nozzle to plate distance 0.5, 1 and 2. They concluded that the position of the second peak of Nusselt number that is observed at the low nozzle to plate distance coincides with enhancement of wall-normal turbulent heat-flux near the wall. Another Direct numerical simulation was done by Jaramillo et al. [10]. They simulated confined impinging slot jet at a fixed Reynolds number 20000 and constant dimensionless nozzle to plate 4. They reported coincidence of secondary Nusselt number peak and enhancement of the wall-normal turbulent heat flux near the impingement wall. Goldstein et al. [11] experimentally measured Nusselt number and recovery factor for unconfined axisymmetric impinging jet at Reynolds number variation of 61000-124000 and dimensionless nozzle to surface range 2-12. They indicated that recovery factor behavior is independent of Reynolds number but dependent on the nozzle to surface distance. The local minima in recovery factor distribution and local maxima in Nusselt number distribution over impinging plate were reported at small nozzle to plate distance at dimensionless radial distance around two. Limaye et al. [12] experimentally investigated the effects of Mach number variation at axisymmetric unconfined impinging jet at different Reynolds numbers and nozzle to plate distances. Based on their conclusion, Nusselt number at all radial distance on the impinging plate is increased by increasing Reynolds number at all nozzle to plate distance. Recovery factor at stagnation point is unity for dimensionless nozzle to

plate distance lower than 6 and greater than unity for higher nozzle to plate distance.

As mentioned above, many investigations have been done on the turbulent impinging jets. However, at this paper, the assessment of the Spalart-Allmaras turbulent model and the effect of compressibility are studied. The object of the investigation the nozzle to plate distance is to demonstrate the assessment of predicting heat transfer by Spalart-Allmaras model and Nusselt number behavior over impinging plate. Turbulent intensity at nozzle exit is another important factor in impinging jet physics, the effect of this parameter is vital in flows that generation of turbulence is low. The effect of this parameter is investigated at Reynolds number 5000 at this paper. The effect of various Mach numbers at a constant Reynolds number 133000 is classified and discussed at this study. In spite of the importance, the effect of compressibility is less mentioned in literature. Investigation the effect of compressibility at high Reynolds number for confined impinging jet is novelty of this paper.

## II. GOVERNING EQUATIONS

Two-dimensional compressible continuity, momentum and energy equations are governed flow in this study. The flow transport and thermodynamic properties are assumed constant during solution process. Turbulence viscosity is computed by Spalart-Allmaras turbulent model [13]. Simulation is done by employment of the cell center finite volume scheme. Every grid cell is defined as a control volume in this method, and flow properties are stored at the center of the grid. Inviscid and viscous fluxes for governing equations and convective and diffusive fluxes for turbulent transport equation must be computed at each face of the control volume. Then fluxes are integrated over cell to define flow properties at the center of the control volume. Governing and turbulent transport equations are discretized separately in time and space based on the method of lines. Inviscid fluxes are computed based on AUSM<sup>+</sup>. More details can be found in reference [14].

Green's theorem is used to compute first derivative of velocity's components, temperature and transported variable at turbulent model at the faces of every grid cell. After the derivatives are computed, viscous fluxes and turbulent model fluxes can be calculated at each face. Simple explicit method is employed for discretization in time after the fluxes integrated over the control volume. All above steps with using proper boundary condition are repeated until convergence is achieved in numerical domain. Ghost cells are used to impose proper boundary condition for numerical simulation. At upper and lower wall, no slip condition and constant temperature for lower wall and adiabatic condition for upper wall are imposed. Fig. 1 depicts the numerical domain and coordinate system for impinging jet over the flat plate. Structure grid is used to divide computational domain to adequate cells. At exit boundary, atmospheric pressure is set, at the jet inlet, uniform velocity, constant temperature and proper turbulent intensity are used, and at the symmetry line, the first component of velocity and the first derivative of temperature, pressure and turbulent model variable are vanished.

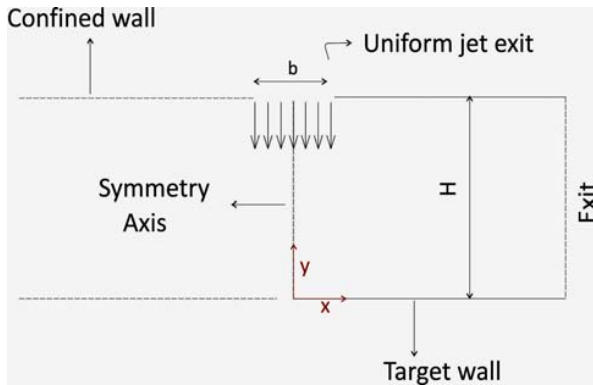


Fig. 1 Computational domain and coordinate system for flat plate as impinging plate

To compute Nusselt number at high Reynolds number and various Mach number, first the thermal boundary for impinging plate is set adiabatic and distribution of adiabatic temperature at surface is obtained, then a real case with constant temperature for impinging wall is simulated. It is notable that static temperature of jet is set lower than ambient temperature and total temperature of jet is set to equal ambient temperature.

To validate the present numerical method, various standard tests have been done in laminar and turbulent regime. Flow in subsonic/supersonic nozzle, impact of supersonic flow to closing and opening edges and consequently formation of oblique shock and expansion waves, shock tube problem and formation of bow shock in front of a cylinder at supersonic flow are simulated and compared with analytical solutions and experimental results to validate the inviscid part of the numerical method. Laminar flow over a flat plate at constant free stream velocity and fully developed flow in a channel are selected problems for validation of viscous fluxes discretization method. Finally, turbulent flow over a flat plate and turbulent free jet are chosen to verify implementation and discretization method of turbulent model. Laminar impinging jet flow characteristics containing Nusselt number and skin friction coefficient are simulated and compared with available results at literatures. At the next section, validation and assessment of Spalart-Allmaras turbulent model at different nozzle to plate distances are presented.

### III. RESULTS AND DISCUSSION

As mentioned in literature review, many simulations have been done by using different RANS models to predict flow characteristics on impinging jets, but Spalart-Allmaras have not been implemented to turbulent impinging jets simulation, or maybe, this model results have not been presented as widely as other RANS model. At this section, confined turbulent impinging slot jet upon a flat plate is simulated at Reynolds number 20000 and at different dimensionless nozzle to surface distances ( $H/b$ ) 4 and 9.2. These distances are chosen because other numerical results and experimental data are available for comparison; Moreover, the assessment of Spalart-Allmaras is verified at both cases where impinging jet

is among its potential core and where impinging jet is out of its potential core.

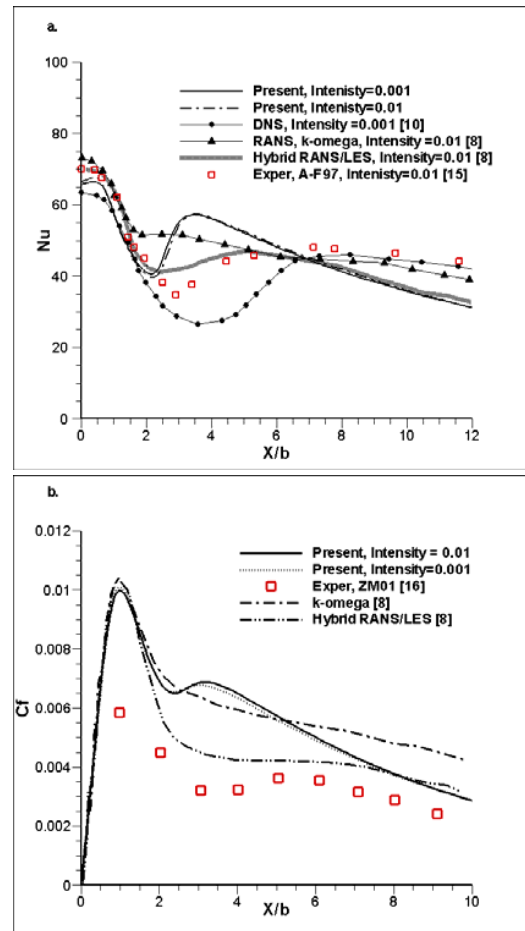


Fig. 2 Comparison for flow characteristics over impinging plate at  $Re = 20000$  and  $H/b=4$

Figs. 2 and 3 show the comparison of present result with available numerical and experimental data from literatures. The Spalart-Allmaras predicted the heat transfer at both distances are reasonable. The  $k-\omega$  results at both cases, except at stagnation point, are controversial. At low nozzle to plate distance, based on the other results from literatures, Nusselt number has a second peak. Transition from laminar to turbulent boundary layer or augmentation of turbulent intensity after stagnation point on the flow are mentioned reasons at literatures for second peak of Nusselt number at short nozzle to impinging plate distance. However, at high nozzle to plate distance, shear layer penetrates the jet centerline and at stagnation point, flow is already turbulent and the second peak of Nusselt number vanishes. Based on the discussion of reference [8,10], at  $H/b = 4$ , jet centerline is laminar, so all RANS model can predict stagnation Nusselt number accurately, but it is obvious from Fig. 2 that  $k-\omega$  cannot capture the second peak of heat transfer definitely because of low mixing at shear layer both at impinging jet and wall jet. On the contrary, the Spalart-Allmaras can predict

secondary peak of heat transfer. At  $H/b = 9.2$ , the second peak of the Nusselt number is not observed, and the heat transfer monotonously decreased from stagnation point. Nevertheless, the  $k-\omega$  predicts the second peak for Nusselt number because of slow spreading of jet and under-estimated turbulent intensity at shear layers of impinging jet and wall jet [8]. The Spalart-Allmaras model can simulate flow behavior reasonably in respect to other numerical simulation methods.

The Spalart-Allmaras simulation of skin friction coefficients at both distances are in good agreement with hybrid RANS/LES results. Over-predicted skin friction coefficient by  $k-\omega$  at large nozzle to plate distance is related to over-estimate the length of potential core and under-estimate turbulent intensity and mixing by this model at large distance, but at lower distance the results corresponds reasonably with other simulations. The Spalart-Allmaras can predict flow behavior in the same accuracy with hybrid RANS/LES method that is presented at reference [8].

Fig. 4 compares the Nusselt number for impinging jet upon a flat plate at Reynolds number 5000 and dimensionless distance 4 for three different turbulent intensities 1%, 5% and 10% at nozzle exit. It is clear from the figure that turbulent intensity does not affect heat transfer, maybe, because of two-dimensional simulation that has been done at this study and negation the effect of three-dimensional real turbulence. Turbulent intensity has key role in flow that generating turbulence is low but at impinging jet physics, high turbulent generation is observed at numerical domain (Turbulent viscosity related to laminar viscosity is around 187 at  $Re = 5000$  and 744 for  $Re = 20000$  at  $H/b = 4$  and 1260 at  $H/b = 9.2$ ).

Figs. 5 and 6 compares heat transfer and dimensionless adiabatic temperature over impinging plate for various Mach numbers at fixed Reynolds number 133000 and dimensionless distance 4. The recovery factor at stagnation point is around unity for all Mach numbers that is expectable because of short nozzle to plate distance ( $H/b = 4$ ). At large nozzle to plate distance, stagnation recovery factor for round jet is reported more than unity due to more entrainment of hot air. Minimum recovery factor occurs at dimensionless distance 2 related to stagnation point. This behavior is also expected for short nozzle to plate distance and this phenomenon attributes to vortex rings in shear layer of the jet that is among its potential core, and energy separation that is caused by minimum energy at center of the vortex [11].

Position of second peak on Nusselt number coincides with the position of local minimum of recovery factor. This behavior was observed by Goldstein et al. [11] too. Enhancement of heat transfer due to vortex ring can be reported as the reason of this coincidence. It should be mentioned that the second peak of Nusselt is higher than stagnation point Nusselt number, this extraordinary maximum was reported by Goldstein et al. [11] again for short nozzle to surface distance. Stagnation Nusselt number is increased with increasing Mach number monotonously from 210 for  $M = 0.3$  to 260 for  $M = 0.8$ . Investigations the effect of high nozzle to plate distance to classify the effect of compressibility at confined impinging jet can be complete the present study.

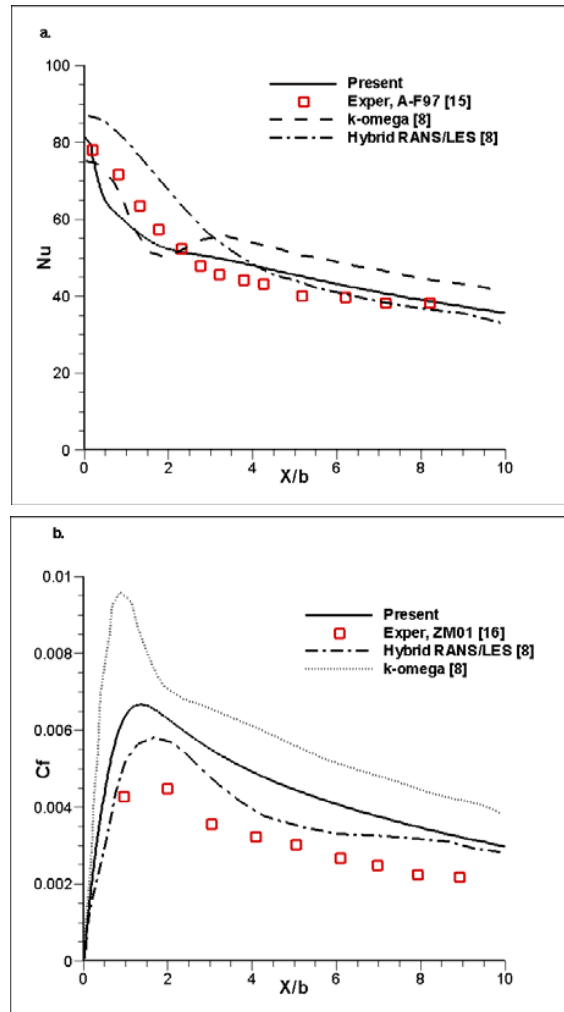


Fig. 3 Comparison for flow characteristics over impinging plate at  $Re = 20000$  and  $H/b = 9.2$

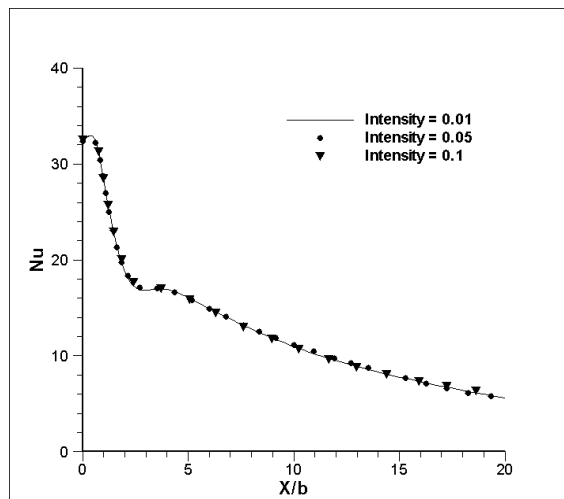


Fig. 4 The effect of turbulent intensity for distribution of Nusselt number at  $Re = 5000$ ,  $H/b = 4$

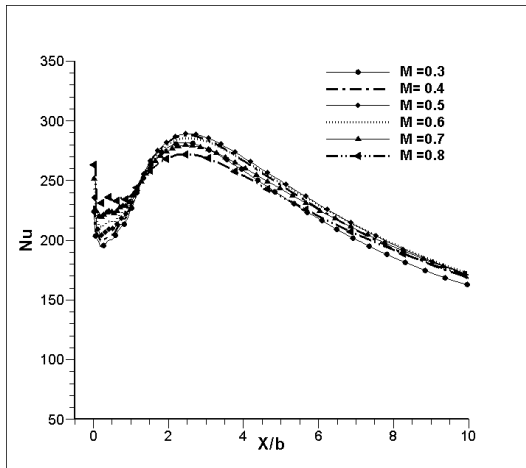


Fig. 5 Comparison for Nusselt number distribution over impingement plate at various Mach numbers at  $Re=133000$  and  $H/b=4$

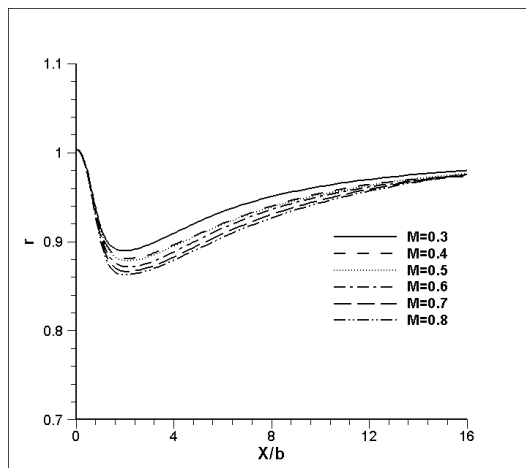


Fig. 6 Comparison for recovery factor distribution over impingement plate at various Mach number at  $Re=133000$  and  $H/b=4$

#### IV. CONCLUSION

A comprehensive numerical study of the effects of different parameters on impinging turbulent confined slot jets has been carried out at this study. Effects of nozzle exit's turbulent intensity, nozzle to impinging plate distance, Reynolds number and compressibility are investigated. Various Mach number 0.3-0.8 at a constant high Reynolds number 133000 is considered to clarify the effect of compressibility for complex impinging jet flow. A compressible finite volume solver accompanies by one equation Spalart-Allmaras turbulent model are implemented to simulate flow behavior at this study. Results prove the assessment of Spalart-Allmaras model to prediction of stagnation Nusselt number at nozzle to plate distance in the range of jet potential core length and out of the potential core. In addition, the used model can capture second peak of the Nusselt number along the flat plate at short nozzle to plate distances. The position of second peak of Nusselt number differs from experimental result, but other numerical simulation results have this vital discrepancy with

each other and experimental results too. Turbulent intensity at nozzle exit does not play a vital rule at two-dimensional numerical simulation that has been done at this study; this inefficiency is caused by producing high turbulence in numerical domain. Two-dimensional simulation can be other reasons to nullify the effect of nozzle exit turbulent intensity because turbulent three-dimensional effects cannot be resolved at two-dimensional simulation. The effect of various Mach number at a constant Reynolds number for confined impinging jet upon a flat plate that is not mentioned and not classified at the previous literatures is presented at this study. The flow behavior is like to axisymmetric unconfined impinging jet results that were mentioned previously at literature. However, to complete comparison and to define remarkable discrepancy between to confined and unconfined cases, investigations the effect of different nozzle to plate distances are programed for future work.

#### REFERENCES

- [1] R. Viskanta, "Heat transfer to impinging isothermal gas and flame jets," *Experimental Thermal and Fluid Science*, vol. 6, pp. 111-134, 1993.
- [2] R. Gardon, J.C. Akfirat, "The role of turbulence in determining the heat transfer characteristics of impinging jets," *International Journal of Heat and Mass Transfer*, vol. 8, pp. 1261-1272, 1965.
- [3] E. Baydar, "Confined impinging air jet at low Reynolds numbers," *Experimental Thermal and Fluid Science*, vol. 19, pp. 27-33, 1999.
- [4] M. Behnia, S. Parneix, Y. Shabany, P.A. Durbin, "Numerical study of turbulent heat transfer in confined and unconfined impinging jets," *International Journal of Heat and Fluid Flow*, vol. 20, pp. 1-9, 1999.
- [5] T.H. Park, H.G. Choi, J.Y. Yoo, S.J. Kim, "Streamline upwind numerical simulation of two-dimensional confined impinging slot jets," *International Journal of Heat and Mass Transfer*, vol. 46, pp. 251-262, 2003.
- [6] T.S. O'Donovan, D.B. Murray, "Jet impingement heat transfer-Part I: Mean and root-mean-square heat transfer and velocity distribution," *International Journal of Heat and Mass Transfer*, vol. 50, pp. 3291-3301, 2007.
- [7] F. Beaubert, S. Viazzo, "Large eddy simulation of plane turbulent impinging jets at moderate Reynolds numbers," *International Journal of Heat and Fluid Flow*, vol. 24, pp. 512-519, 2003.
- [8] S. Kubacki, E. Dick, "Simulation of plane impinging jets with  $k-\omega$  based hybrid RANS/LES models," *International Journal of Heat and Fluid Flow*, vol. 31, pp. 862-878, 2010.
- [9] H. Hattori, Y. Nagano, "Direct numerical simulation of turbulent heat transfer in plane impinging jet," *International Journal of Heat and Fluid Flow*, vol. 25, pp. 749-758, 2004.
- [10] J.E. Jaramillo, F.X. Trias, A. Gorobets, C.D. Perez-Segarra, A. Oliva, "DNS and RANS modeling of a turbulent plane impinging jet," *International Journal of Heat and Mass Transfer*, vol. 55, pp. 789-801, 2012.
- [11] R.J. Goldstein, A.I. Behbahani, K. Kiger Heppelmann, "Streamwise distribution of the recovery factor and the local heat transfer coefficient to an impinging circular air jet," *International Journal of Heat and Mass Transfer*, vol. 29, pp. 1227-1235, 1986.
- [12] M.D. Limaye, R.P. Vedula, S.V. Prabhu, "Local heat transfer distribution on a flat plate impinged by a compressible round air jet," *International Journal of Thermal Sciences*, vol. 49, pp. 2157-2168, 2010.
- [13] P.R. Spalart, S.R. Allmaras, "A one equation turbulence model for aerodynamic flows," *La Recherche Aerospaciale*, vol. 1, pp. 5-21, 1994.
- [14] Meng-Sing Liou, "A sequel to AUSM," *Journal of Computational Physics*, vol. 129, pp. 364-382, 1996.
- [15] S. Ashforth-Frost, K. Jambunathan, C.F. Whitney, "Velocity and turbulence characteristics of a semiconfined orthogonally impinging slot jet," *Experimental Thermal Fluid Science*, vol. 14, pp. 60-67, 1997.
- [16] J. Zhe, V. Modi, "Near wall measurements for a turbulent impinging slot jet," *Transactions of ASME, Journal of Fluid Engineering*, vol. 123, pp. 112-120, 2001.